Ti_3Al基合金瞬间液相扩散连接接头组织与力学性能

谷晓燕[1], 孙大千[1], 任振安[1], 刘 力[2], 段珍珍[2]
(1. 吉林大学 汽车材料国家重点实验室, 长春 130025; 2. 长春轨道客车股份有限公司, 长春 130062)

摘 要: 采用 TiZrNiCu合金作为中间层材料研究了 Ti_3Al基合金的瞬间液相扩散连接, 采用扫描电镜(SEM)、能谱仪(EDS)、X射线衍射仪(XRD)及电子万能试验机研究了接头的组织结构与力学性能. 结果表明, 采用 TiZrNiCu作为中间层可以实现 Ti_3Al基合金的 TLP扩散连接, 能形成完整的接头. 较高的连接温度和较长的连接时间有利于获得成分和组织较为均匀的接头. 随着连接温度的提高和连接时间的延长, 接头连接区宽度增大, 反应层数量减少. 当连接温度为 900 ℃, 连接时间为 60 min时, 接头组织主要为钛固溶体, Ti_3Al和 Ti_2Cu. 接头抗剪强度最高, 可达 420.1 MPa.

关键词: Ti_3Al基合金; 瞬间液相扩散连接; 组织; 抗剪强度
中图分类号: TG456.9 文献标识码: A 文章编号: 0253-360X(2010)05-0045-04

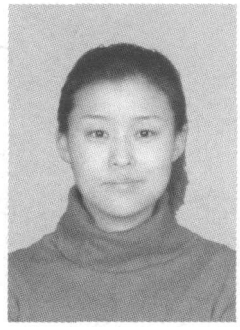

谷晓燕

0 序 言

近年来, Ti_3Al基合金以其较高的高温强度、弹性模量、抗氧化性和较低的密度引起人们的极大关注[1-5]. 但该类合金在室温条件下塑性较低, 限制了其广泛的应用. 添加 Nb, V和 Mo等合金元素可以稳定 β相, 从而提高 Ti_3Al基合金的室温塑性[6-7]. 因此, Ti_3Al-Nb合金作为一种新型、轻质、中高温结构材料, 具有良好的综合性能, 在航空、航天工业中具有较大的工程应用潜力.

任何先进材料的广泛应用, 很大程度上取决于材料的加工制造技术. 焊接(连接)技术成为制约 Ti_3Al-Nb合金应用的主要因素之一. 文中对 Ti_3Al-Nb合金瞬间液相(TLP)扩散焊接头的组织与力学性能进行了研究, 为改善该合金的连接质量提供试验数据和必要的理论依据.

1 试验方法

试验用母材为 Ti_3Al合金, 由 α_2相和 $\beta/B2$相组成(图 1). 其中, α_2相呈球形, 基体主要为层片状次生 α_2相和灰色的 $\beta/B2$相. 焊前采用电火花线切割将母材制备成尺寸为 7 mm×7 mm×3 mm的试样, 选用 TiZrNiCu合金箔作为中间层材料, 中间层厚度为 30 μm, 其化学成分(原子分数)为 51% Ti, 35% Cu, 9% Ni和 5% Zr.

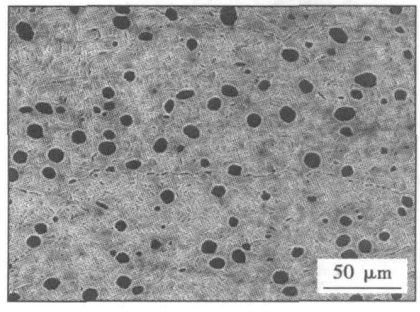

图 1 母材微观组织形貌
Fig. 1 Microstructure of base material

采用 VQB-10Wd真空加热炉对 Ti_3Al基合金进行 TLP扩散连接, 连接过程中真空度不低于 10^{-3} Pa. 采用 JSM-5600型扫描电镜及 Link ISIS300型能谱仪分析接头的组织和成分, 采用 D/Max 2500型 X射线衍射仪分析接头的相结构, 采用 MTS810电子万能试验机测试接头的抗剪强度.

2 试验结果与讨论

2.1 Ti_3Al基合金 TLP连接接头的成分与组织

图 2为连接温度 850 ℃, 连接(保温)时间 1 min时 Ti_3Al基合金 TLP连接接头组织形貌与元素分

收稿日期: 2009-12-16
基金项目: 吉林大学科学前沿与交叉学科创新基金资助项目(200903021)

布. 图 2b中各点对应于图 2a中的十字标识. 从图 2a中可以看到, 接头连接区由 A, B和 C三个反应层组成. 在连接过程中, TiZrNiCu中间层已经熔化, C层宽度接近于中间层合金的初始厚度 (30 μm), 连接区宽度约为 50 μm. 由此可知, 在连接过程中, 母材/中间层界面发生了明显的互扩散. 由能谱分析结果可知, C层中 Cu, Ni和 Zr元素的含量比较高, 接近于中间层材料的原始成分, 并且 Ti, Al和 Nb元素含量有所提高, 这主要是由于固、液相之间浓度梯度的存在使母材中 Ti, Al和 Nb元素向液相中扩散, 同时液相中的 Cu, Ni和 Zr元素也会向固相母材中扩散. 元素的互扩散使得在母材/液相层界面靠近母材一侧产生扩散层 A层, 中间层一侧产生扩散层 B层. 另外, 从图 2a可以看到, 在连接区还存在白色的圆形区域, 能谱分析表明这些区域 Ti, Al和 Nb元素含量较多.

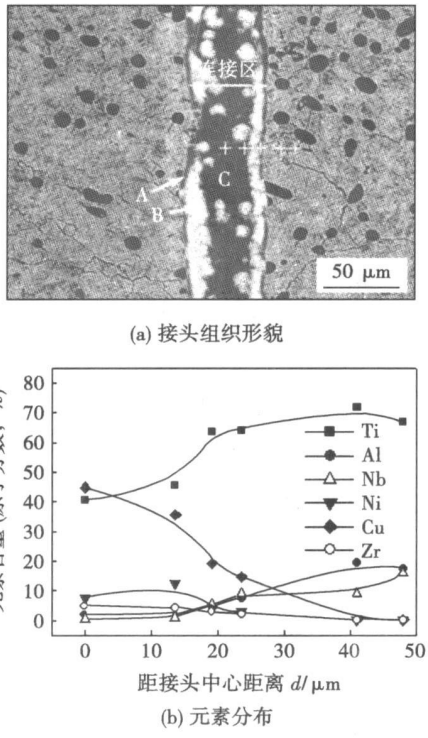

图 2 连接条件为 850 ℃×1 min时接头组织形貌与元素分布

Fig. 2 Microstructure and chemical compositions of joint produced at 850 ℃×1 min

当连接温度提高到 880 ℃时, Cu, Ni和 Zr元素的高浓度区域缩小, 扩散层 B宽度增加; 整个连接区 Ti元素含量升高, Cu元素含量降低, 如图 3所示. 这主要是由于随着连接温度的升高, 原子扩散系数增大, 使得扩散速度增大.

连接温度为 900 ℃, 连接时间为 1 min时, 接头

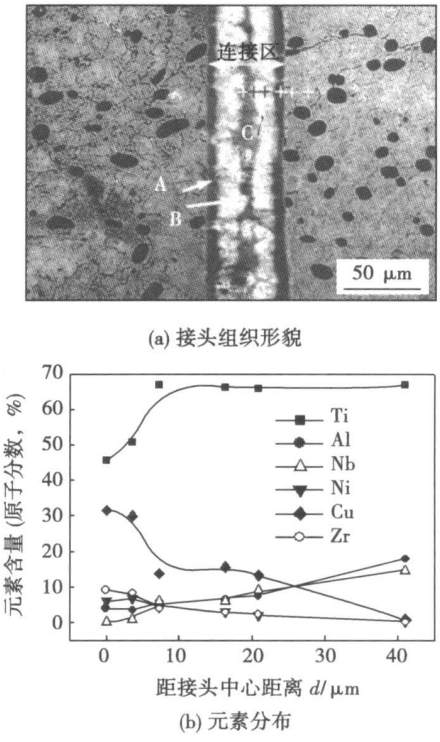

图 3 连接条件为 880 ℃×1 min时接头组织形貌与元素分布

Fig. 3 Microstructure and chemical compositions of joint produced at 880 ℃×1 min

中液相已经开始等温凝固, C层宽度逐渐减小, 约为 17.8 μm. A层和 B层两个反应层之间的界面消失. 由 Ti-Cu二元相图[8]可知, Ti_2Cu_4不断从液相中析出, 多余的溶质元素 Ni被排到残余液相中, 使得液相中 Ni元素含量升高, 如图 4所示. 由于化学成分的差异, 等温凝固析出的固相和与之相邻的固相母材之间会发生固相扩散, 生成更加稳定的化合物, 这主要取决与该化合物热力学和动力学因素. 由于连接 (保温) 时间没有达到足够长, 使得保温结束时, 接头中存在没有完成等温凝固的液相, 保温结束后的冷却过程中, 接头中的残余液相会发生一系列的反应. 温度降低到 890 ℃时, 残余液相 (L) 与 Ti_2Cu_4发生包晶反应 ($Ti_2Cu_4 + L \rightarrow TiCu_2$), 温度降到 875 ℃时, 残余液相经过共晶反应 ($L \rightarrow TiCu_2 + \beta Ti$) 转变为 $TiCu_2 + \beta Ti$.

图 5为连接温度 900 ℃, 连接时间 30 min时接头的组织形貌与元素分布, 随着连接时间的延长, 液相区宽度进一步减小 (约为 6.4 μm), 等温凝固析出的固相和与之相邻的母材之间的元素扩散使得整个连接区宽度增大.

连接温度为 900 ℃, 连接时间为 60 min时 (图 6), C层从接头中消失, 表明等温凝固过程已经结束. 连接区宽度进一步增大, 整个连接区形成均

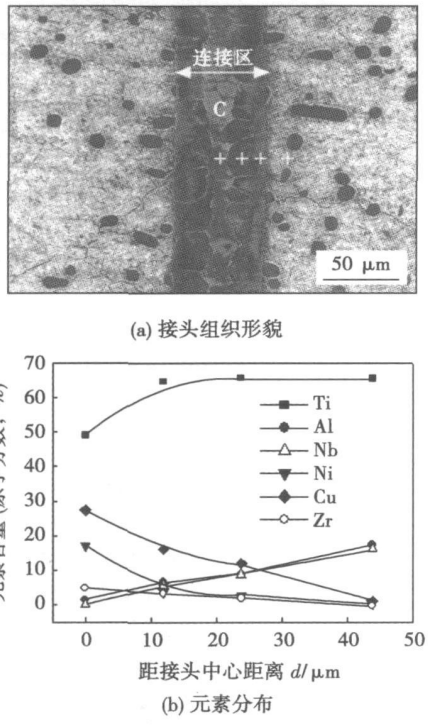

图 4　连接条件为 900 ℃×1 min 时接头组织形貌与元素分布

Fig. 4　Microstructure and chemical compositions of joint produced at 900 ℃×1 min

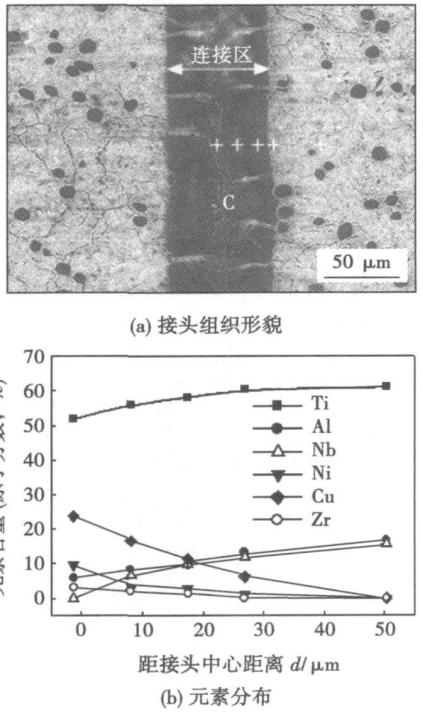

图 5　连接条件为 900 ℃×30 min 时接头组织形貌与元素分布

Fig. 5　Microstructure and chemical compositions of joint produced at 900 ℃×30 min

匀一致的针状组织. 从能谱成分来看，此时接头中 Ti、Al、Nb、Cu、Ni和 Zr元素分布比较均匀.

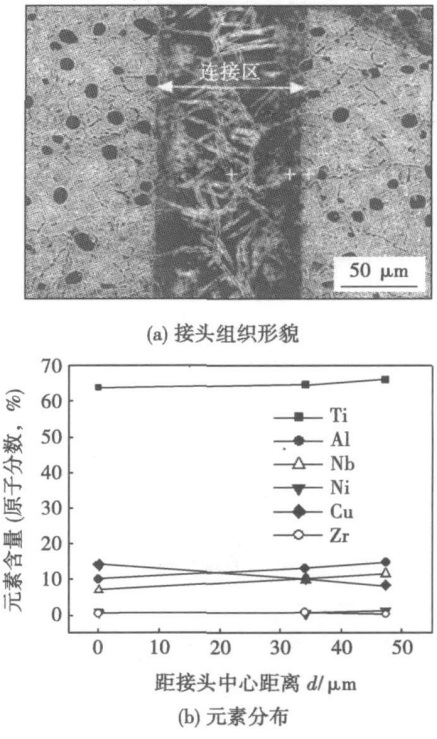

图 6　连接条件为 900 ℃×60 min时接头组织形貌与元素分布

Fig. 6　Microstructure and chemical compositions of joint produced at 900 ℃×60 min

图 7为 Ti_3Al基合金 TLP连接接头的 XRD分析结果. 连接温度为 850 ℃，连接时间为 1 min时，接头的组织主要为 Ti_3Cu_4、Ti_2Cu和 $Ti(Ni,Cu)$. 连接温度为 900 ℃，连接时间为 60 min时，接头的组织主要为钛固溶体、Ti_3Al和 Ti_2Cu.

综上所述，当连接时间比较短时，保温结束时接头中存在残留液相；连接时间较长时，由于接头中液相已经完全等温凝固，接头成分比较均匀. 接头连接区宽度、扩散反应层的数量以及元素的分布随着连接温度和连接时间的变化而变化. 连接温度较低、连接时间较短时，接头由三个反应层组成；随着连接温度的提高和连接时间的延长，扩散层消失，连接区组织趋于均匀. 随着连接温度的提高和连接时间的延长，接头中各元素的分布趋于均匀.

2.2　Ti_3Al基合金 TLP连接接头的抗剪强度

连接时间为 1 min，连接温度分别为 850、900、950 ℃时，接头的抗剪强度变化范围为 171.5～392.2 MPa；连接温度为 900 ℃，连接时间分别为 1、15、30和 60 min时，接头抗剪强度变化范围为 132.2～420.1 MPa(表 1). 所有接头均断裂在连接区，表明连接区为接头强度的薄弱区域.

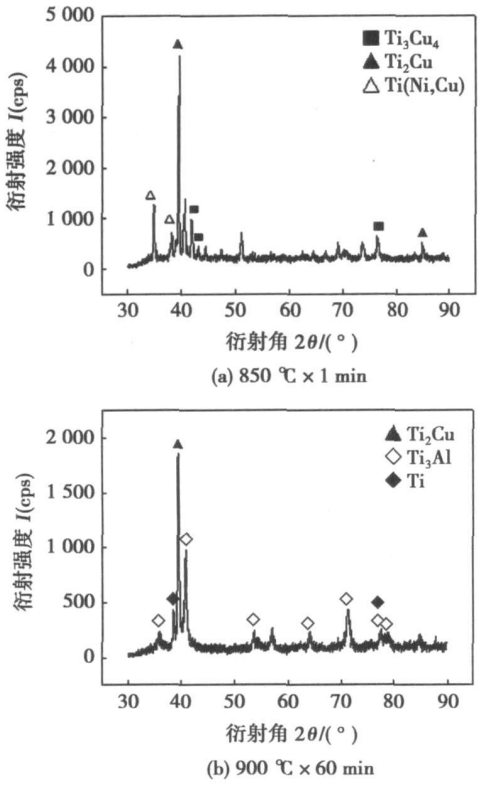

图 7 接头 XRD分析

Fig. 7 XRD analysis of joints

表 1 Ti_3Al基合金 TLP连接接头抗剪强度

Table 1 Shear strength of Ti_3Al based alloy joints

连接时间 t/min	抗剪强度 R_τ/MPa		
	连接温度 850 ℃	连接温度 900 ℃	连接温度 950 ℃
1	196.2	392.2	171.5
15	—	132.2	—
30	—	230.8	—
60	—	420.1	—

3 结 论

(1)采用 Ti/Zr/Ni/Cu合金作为中间层可以实现对 Ti_3Al基合金的 TLP扩散连接,能形成完整的接头.

(2)随着连接温度的提高和连接时间的延长, Ti_3Al基合金瞬间液相扩散连接接头连接区宽度增大,反应层数量减少,其成分和组织趋于均匀.当连接温度为 900 ℃,连接时间为 60 min时,接头组织主要为钛固溶体 Ti_3Al和 Ti_2Cu.

(3)当连接温度为 900 ℃,连接时间为 60 min时, Ti_3Al基合金瞬间液相扩散连接接头抗剪强度最高,可达 420.1 MPa.

参考文献:

[1] Kim J S, Shin D H, Chang Y W, et al. Constitutive analysis on superplastic deformation mechanisms of two-phase Ti_3Al-xNb alloy [J]. Materials Science and Engineering A, 2005, 394(1—2): 117—125.

[2] Dutkiewicz J, Maziarz W, Heinrich H, et al. Structure of Ti-Al-Nb intermetallics produced by mechanical alloying and hot-pressing techniques [J]. Materials Chemistry and Physics, 2003, 81(2—3): 414—416.

[3] Ward-Close C M, Minor b R, Doorbar b P J. Intermetallic-matrix composites-a review [J]. Intermetallics, 1996, 4(3): 217—229.

[4] Yoo M H, Maruyama K, Yamaguchi M, et al. Effects of lamellar boundary structural change on lamellar size hardening in TiAl alloy [J]. Acta Materialia, 2004, 52(17): 5185—5194.

[5] Maurice V, Despert G, Zanna S, et al. XPS study of the initial stages of oxidation of α_2-Ti_3Al and γ-TiAl intermetallic alloys [J]. Acta Materialia, 2007, 55(10): 3315—3325.

[6] Yang K L, Huang J C, Wang Y N. Phase transformation in the β phase of super-α_2 Ti_3Al base alloys during static annealing and superplastic deformation at 700—1 000 ℃ [J]. Acta Materialia, 2003, 51(9): 2577—2594.

[7] Dutkiewicz J, Maziarz W, Scholz R. Structure changes during mechanical alloying of TiAlNb alloys [J]. Inzynieria Materialowa, 2001, 123(4): 299—302.

[8] 虞觉奇, 易文质, 陈邦迪, 等. 二元合金状态图集 [M]. 上海: 上海科学技术出版社, 1987.

作者简介:谷晓燕,女,1979年出生,博士,讲师.主要从事新材料连接的研究工作.发表论文 9篇.

Email: sundq@jlu.edu.cn

proach for the sub-system of plasma jet generation was presented in this paper based on the rule sets supervision and multi-model adaptive control system structure.

Key words: plasma spraying; plasma jet morphology; intelligent control; data mining; clustering analysis

Brazing of aluminum matrix composites SiC_p/ZL101 to Kovar alloy 4J29 NIU Jitai[1,2], LU Jinbin[1], MU Yunchao[1], LUO Xiangwei[3] (1. Department of Materials and Chemical Engineering, Zhongyuan University of Technology, Zhengzhou 450007, China; 2. State Key Laboratory of Advanced Welding Production Technology, Harbin Institute of Technology, Harbin 150001, China; 3. Department of Materials Science & Engineering, Zhengzhou University, Zhengzhou 450002, China). p 37 - 40

Abstract: SiC_p/ZL101 composites containing 55% SiC_p and Kovar alloy 4J29 were chosen as base metals. After being electroplated by Ni on the SiC_p/ZL101, the two materials were brazed by Zn-Cd-Ag as filler metal at the 420 ℃ for 7 min. Moreover, the interfacial microstructures and fracture appearances were investigated by SEM and EDS. The results show that the electroplated Ni on the surface of SiC_p/ZL101 can improve the filler's wettability to the composite material. There are transition layers not only between the filler and Kovar alloy, but also between the filler and the electroplated Ni layer, which shows the filler metal, the electroplated Ni layer, the composites and Kovar alloy can realize metallurgically joining by diffusion. The fracture analysis shows that the fracture happens inside the composites near the electroplated Ni layer.

Key words: aluminum matrix composites; Kovar alloy; brazing Ni electroplating

Analysis of chemical reaction on weld pool surface in activating TIG welding of aluminum alloys HUANG Yong, FAN Ding, SHAO Feng (State Key Laboratory of New Non-ferrous Metal Materials, Lanzhou University of Technology, Lanzhou 730050, China). p 41 - 44

Abstract: For activating TIG welding of aluminum alloys, including A-TIG welding, FB-TIG welding and FZ-TIG welding, the analysis of chemical reaction between the activating fluxes and the weld pool metal has great significance to certain the feasibility of these welding processes and instruct the developments of activating fluxes. Through the XRD analysis of weld surface slag, the chemical reaction thermodynamics was calculated based on functional determinant of Gibbs' Free Energy, and the chemical reaction on welding pool was analyzed. It is found that, for the FZ-TIG welding, with multi-component flux FZ108 developed by authors as central region flux and SiO_2 as outer region flux, the endothermic reactions between flux FZ108 and the welding pool metal can constrict the arc and increase weld penetration. For the A-TIG welding with flux FZ108, the few absorbed heat or the released heat of the chemical reactions has small influence on the arc. For the FB-TIG welding with flux SiO_2, the chemical reaction between the flux and the weld pool metal and its surface oxide film does not happen, and the arc is not affected through these chemical reactions.

Key words: aluminum alloy; A-TIG welding; activating flux; chemical reaction; arc constriction

Microstructures and mechanical properties of transient liquid phase bonded Ti_3Al based alloy joints GU Xiaoyan[1], SUN Daqian[1], REN Zhen'an[1], LIU Li[2], DUAN Zhenzhen[2] (1. Key Laboratory of Automobile Materials, Jilin University, Changchun 130025, China; 2. Changchun Railway Vehicles Co., LTD., Changchun 130062, China). p 45 - 48

Abstract: Microstructure and mechanical properties of Ti_3Al based alloy joints bonded by transient liquid phase bonding were studied by scanning electron microscope (SEM), energy dispersive X-ray spectroscope (EDS), X-ray diffraction (XRD) and universal test machine. The results show that the integrated joints were prepared by TLP bonding with the TiZrNiCu alloy interlayer. The high bonding temperature and long bonding time help to obtain the joints with uniform composition and microstructure. With bonding temperature and bonding time increasing, the width of the bonding zone increases and reaction zones decreases. When bonding time is 60 min at bonding temperature of 900 ℃, the joint microstructure consists of Ti solid solution, Ti_3Al and Ti_2Cu and the joint strength of 420 MPa can be obtained.

Key words: Ti_3Al based alloy; transient liquid phase diffusion bonding; microstructure; shear strength

CoNiCrAlY alloy deposited on surface of SCH13 steel by laser cladding ZHANG Song[1], WANG Mingsheng[1], ZHANG Kaixiang[1], ZHANG Chunhua[1], YAN Yonggen[2] (1. School of Materials Science and Engineering, Shenyang University of Technology, Shenyang 110023, China; 2. Baoshan Iron & Steel Co., Ltd., Shanghai 201900, China). p 49 - 52

Abstract: The surface of SCH113 steel was deposited with CoNiCrAlY alloy by a high power CO_2 laser. Through, the excellent coatings can be acquired by the optimized process parameters. The micro-structure, composition, hardness and corrosive resistance of the coating were examined by scanning electron microscope (including EDS microanalysis), X-ray diffraetometry, micro thickness meter, wear test machine. The results indicated that the coating of CoNiCrAlY alloy has a good metallurgical combination with SCH13 steel, and the other characteristics such as fine microstructure, no cracks, low dilution rate and the smooth transition of elements at the interface. The coatings were consisted of γ-Co, $FeCr_{0.29}Ni_{0.16}C_{0.06}$, FeNi, CoC_x and $Cr_{23}C_6$ phases. The average microhardness of the coating is 3 times higher than that of the SCH13 steel. Furthermore, the wear resistance of laser cladded coating is 3.42 times higher than that of the matrix.

Key words: SCH13 steel; laser cladding; CoNiCrAlY alloy coatings; microstructure; property

Electron beam welding of TA15 titanium alloy to 304 stainless steel WANG Ting, ZHANG Binggang, CHEN Guoqing, FENG Jicai (State Key Laboratory of Advanced Welding Production Technology, Harbin Institute of Technology, Harbin 150001, China). p 53 - 56

Abstract: Electron beam welding experiment of TA15 titanium alloy to 304 stainless steel was carried out. Microstructure and micro-hardness distribution of joint were examined. The results showed that the weldability of electron beam welding of TA15 titanium alloy to 304 stainless steel was so poor that many